SSRG International Journal of Mechanical Engineering
ISSN: 2348-8360/ https://doi.org/10.14445/23488360/IJME-V13I7P102

Volume 13 Issue 7, 16-26, July 2026

Original Article

Simulation-Based Ergonomic Comfort Assessment of Truck Drivers using a Digital Human Model

Quoc Hoang Pham[1], Ky Nam Le[2], Van Tu Nguyen[2], Thanh Lam Tran[2*]

[1]*Department of Science, Le Quy Don Technical University, Vietnam.*
[2]*Institute of Vehicle and Energy Engineering, Le Quy Don Technical University, Vietnam.*

[*]*Corresponding Author : thanhlam.tran@lqdtu.edu.vn*

Received: 01 May 2026 Revised: 23 June 2026 Accepted: 08 July 2026 Published: 30 July 2026

Abstract - *This study aims to develop digital human models for a Vietnamese population group using empirical anthropometric data collected from 171 male students aged 20-29 years majoring in automotive engineering at Le Quy Don Technical University. A human body shape estimation method based on two RGB images, captured from the frontal and lateral views, was combined with the parameterized 3D human body model provided by the SMPL-X library to generate the model data. From these data files, key anthropometric parameters were calculated to support the assessment of driver postural comfort during vehicle operation. In addition, the study employed a KAMAZ-6560 truck cabin model and its main cabin components reconstructed from 3D scanning data, thereby determining the geometric dimensions corresponding to the real cabin. Based on the synthesized anthropometric data, three representative models corresponding to the minimum, mean, and maximum body sizes were selected. Siemens NX was then used to perform simulations with the Jack human model and the representative dataset. Driver posture was evaluated according to the comfort-angle criteria proposed by Porter and Gyi. Furthermore, for the original cabin layout, recommendations were proposed for the optimal positions of the seat and pedals when using the mean anthropometric dimensions of the surveyed group. The results show that the current clutch pedal height is 12.8 cm and its inclination is approximately 18° relative to the floor, causing the foot-ankle angle to exceed the comfort limit by about 15°. For the mean anthropometric case, the clutch pedal should be lowered so that the height from the contact point to the floor is within 7-8 cm. For the driver model with a stature of 188 cm, the seat should be moved forward by approximately 10 cm to ensure a comfortable arm working angle during driving.*

Keywords - *Digital Human Model, Vietnamese Anthropometry, Truck Cabin, Postural Comfort Assessment, Ergonomics*.

1. Introduction

To achieve an optimal ergonomic design for drivers in different geographical regions, comprehensive anthropometric data of the target population are essential. Although numerous studies worldwide have reported anthropometric data for European, Asian, and American populations, anthropometric statistics for Vietnamese people used in optimizing driving-space design and evaluating driver comfort remain limited. Along with economic and nutritional development, recent studies (2019-2020) indicate a marked increase in the body size of Vietnamese people [1, 2].

Compared with the 1982-1985 period, Vietnamese working-age males currently have a mean stature of 164.60 ± 5.80 cm, an increase of 4.60 cm, while females have a mean stature of 154.50 ± 4.80 cm, an increase of 4.50 cm. The increase in body mass is even more pronounced: the mean body mass of males is 59.20 kg, an increase of 10.6 kg, and that of females is 50.80 kg, an increase of 6.50 kg [3]. Therefore, there is an urgent need to investigate and develop digital human models that reflect the current anthropometric characteristics of the Vietnamese population.

Anthropometric research on Vietnamese people has a history spanning several decades. Landmark works such as "Biological Constants of Vietnamese People (1975)" by N. T. G. Trong and "Anthropometric Atlas of Vietnamese People of Working Age (1986)" by V. Hung laid the foundation for morphological data on Vietnamese people [4, 5]. Most domestic studies have focused on nutritional and medical assessment, the physical development of pupils and students, or applications in fashion design and general occupational ergonomics [1-3, 6, 8-12]. In addition, studies in Vietnam have mainly addressed static measurements, such as standing height, sitting height, and chest circumference [1-3]. In contrast, automotive cabin design requires dynamic data, including arm reach, joint range of motion during driving, and changes in body morphology during vehicle ingress and egress [7].

At present, Vietnam has only begun to develop 3D avatars for fashion design (CLO3D) [11, 12], while no digital human model has yet fully integrated Vietnamese anthropometric characteristics for testing cabin-space design and assessing driver comfort. Moreover, human body measurements still lack percentile-specific data for automotive cabin design, which must accommodate users ranging from the smallest, such as the 5th-percentile female, to the largest, such as the 95th-percentile male [7]. Although a study has classified the body shapes of middle-aged Vietnamese males (30-60 years) in Ho Chi Minh City based on 32 anthropometric measurements [11], the application of these body-shape categories to determine adjustment ranges for the seat, steering wheel, clutch pedal, accelerator pedal, and brake pedal for Vietnamese users has not been examined in depth [7]. Several studies indicate that Asians in general, and Vietnamese people in particular, often have a longer upper body and shorter lower limbs relative to total stature [7]. Therefore, direct application of SAE standards based primarily on European and American body proportions may introduce errors in the overall cabin layout for Vietnamese users.

Digital Human Models (DHMs) currently used worldwide are highly diverse and can be classified by application purpose, ranging from industrial design and medicine to computer vision. Common DHMs include RAMSIS, which is regarded as a core standard in the automotive industry and is widely used to simulate driving posture, evaluate vision, and assess comfort in vehicle interiors [7, 13, 15, 16, 24-27]. JACK, developed by NASA and the University of Pennsylvania, focuses on human performance simulation and assembly planning in industrial environments. Human Builder is deeply integrated into CAD systems to evaluate accessibility, reach envelopes, and manual operations directly on design drawings [7]. Anybody is a specialized biomechanical model that enables detailed calculations of muscle forces and loads acting on the musculoskeletal system [7].

The assessment of driver ergonomic comfort has been widely conducted using various simulation tools worldwide, including DHM RAMSIS models, MADYMO and CASIMIR models [7, 24, 27], artificial intelligence algorithms such as artificial neural networks [11, 16], and stochastic optimization algorithms [18]. In contrast, this paper adopts a new approach by focusing on static ergonomic evaluation through the integration of 2D images, the SMPL-X library, and the JACK digital human model, with the aim of optimizing the cockpit space and human body joint angles. However, compared with several previous studies, this work has the limitation of addressing only static ergonomics, without considering dynamic ergonomic factors. These include, for example, the effects of vibration and shock transmitted through the suspension system [14, 21, 23] or the biomechanical forces acting on the human body during vehicle acceleration and braking [16].

In addition, this study uses comfort-angle criteria for driving posture as a basis for ergonomic assessment. These criteria are founded on the principle of neutral posture, in which muscle groups remain in their most relaxed state without excessive contraction or stretching [19]. The following Table 1 summarizes the parameters proposed by Porter and Gyi, one of the classic and widely recognized rule sets in automotive ergonomics [22, 23]:

Table 1. Joint-angle comfort parameters according to Porter and Gyi (1998)

No.	Joint location	Observed posture (n = 55)	95% confidence limits
1	Neck inclination angle	30° - 66°	29° - 63°
2	Hip angle	90°- 115°	89° - 112°
3	Knee angle	99° - 138°	103° - 136°
4	Arm flexion angle	19° - 75°	16°- 74°
5	Elbow angle	86°- 164°	80° - 161°
6	Ankle angle	80°- 113°	81° - 105°

These values were developed by Porter and Gyi to reduce pressure on the spinal intervertebral discs and minimize driver fatigue during long-distance driving.

2. Materials and Methods

2.1. Study Subjects

The subjects of this study were Vietnamese males, represented by male students aged 20-29 years from Le Quy Don Technical University. All participants were confirmed to have normal body morphology and health status.

The following formula was used to determine the sample size [8, 11]:

$$n = \frac{t^2 . SD^2}{m^2} \quad (1)$$

Where t is the 95% confidence coefficient, SD is the standard deviation, and m is the allowable error.

Standing height was used to calculate the minimum number of subjects required for measurement. The stature data for Vietnamese males reported in the study "General observations on anthropometric characteristics of Vietnamese people of working age in 2018-2019" indicate that the standard deviation for males aged 20-29 years is SD = 6.00 cm [3].

With an allowable error of 15% of the standard deviation (m = 6 × 0.15 = 0.90 cm) and a 95% confidence level (t = 1.96), the required sample size was n = 171.

IBM SPSS 26 was used to generate the height and body-mass distributions of the study sample as follows:

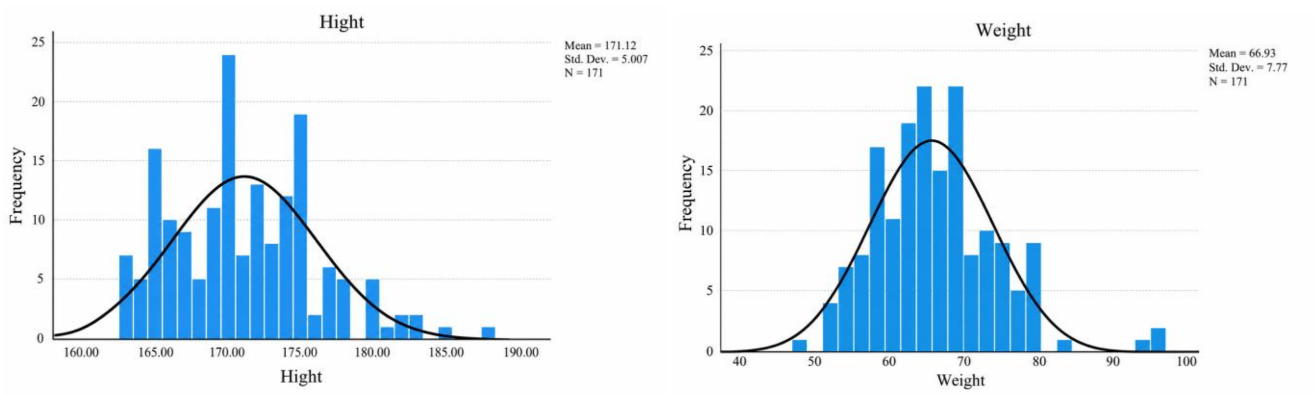

Fig. 1 Height and body-mass data of 171 students from LQDTU

The height data had a mean value of 171.12 cm, a standard deviation of 5.01 cm, and a sample size of N = 171. Thus, the stature of the surveyed group was concentrated mainly around 171.00 cm, with a typical variation of approximately ±5.00 cm.

The mean body mass of the surveyed group was approximately 66.93 kg, with a typical variation of about ±7.77 kg around the mean. In other words, most participants had a body mass of approximately 59-75 kg, which also corresponds to the highest-frequency region in the distribution. The data followed an approximately normal distribution.

2.2. Method for Developing the Digital Human Model

The development of a Digital Human Model (DHM) is an integrated approach combining anthropometric data acquisition, biomechanics, and computer-based techniques to synthesize a complete model. Modern DHM construction is based primarily on two core components: an internal musculoskeletal model, which reproduces postural and movement functions through articulated joints [13, 24, 27, 28], and an external skin-surface model, which provides a realistic appearance and is coupled with the skeletal framework through mathematical algorithms to ensure natural skin deformation during motion. Methods such as the Finite Element Method (FEM) are used to simulate soft tissues, including muscle and fat [13, 28, 29].

The first step in developing the DHM is to collect anthropometric data through static measurements. To ensure dimensional accuracy, this study employed model-based human body shape estimation from two RGB images. This method uses a frontal image and a lateral image captured perpendicular to the frontal plane to obtain body width and depth [36, 38, 39]. First, 2D body joint landmarks are detected using MediaPipe [34]. In parallel, the person is segmented from the background to extract the body silhouette. Instead of reconstructing a free-form 3D body from the segmented images, the system initializes a parameterized SMPL-X (Skinned Multi-Person Linear Model eXpressive) body model using shape parameters (β) and pose parameters (θ), with N = 10475 mesh vertices [9, 30-37].

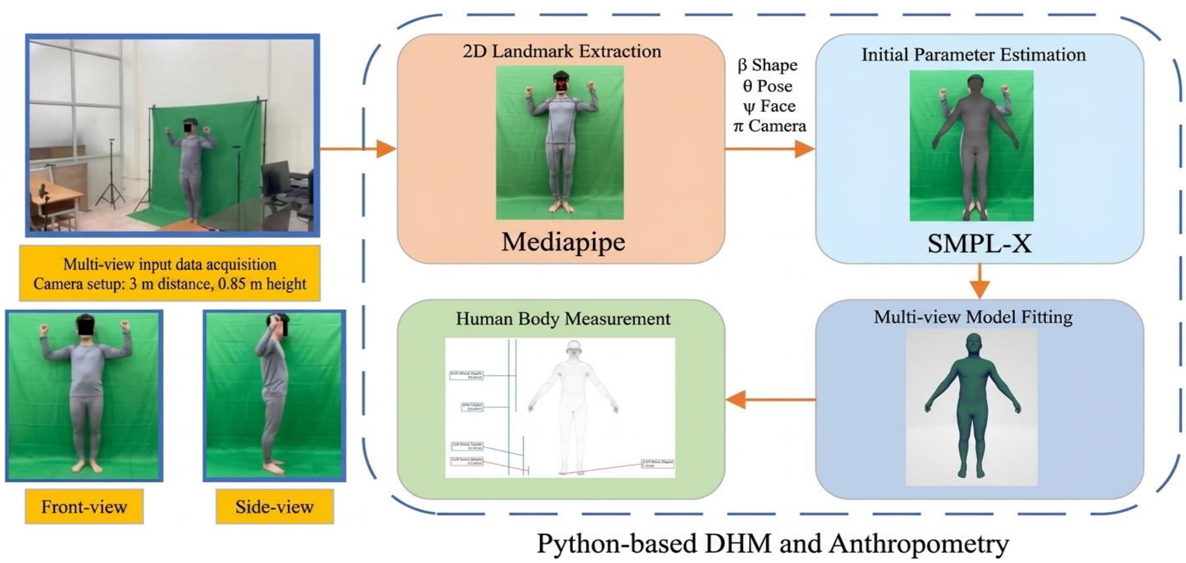

Fig. 2 Human body shape estimation from two RGB images and anthropometric measurement

The model-based fitting approach for human body shape estimation is mathematically formulated as follows:

The SMPL-X model represents the human body through a function $M(\beta,\theta,\psi)$, which maps the input parameters to a 3D mesh. The shape parameter $\beta: \beta \in \mathbb{R}^{10}$represents the coefficients of the first 10 principal components extracted from the human body-shape space. The pose parameter $\theta: \theta \in \mathbb{R}^{3K}$(with K = 54 joints) describes the relative rotations of skeletal joints in the axis-angle representation, and the facial expression coefficient $\psi: \psi \in \mathbb{R}^{|\psi|}$ is also included [34].

Mesh generation: the mesh is generated using the following equations:

$$M(\beta,\theta,\psi) = W\big(T_p(\beta,\theta,\psi), J(\beta), \theta, \mathcal{W}\big)$$
$$T_p(\beta,\theta,\psi) = \bar{T} + B_S(\beta;S) + B_E(\psi;E) + B_P(\theta;P)$$
$$B_S(\beta;S) = \sum_{n=1}^{|\beta|} \beta_n S_n \quad (2)$$

where W is the skinning function; TP is the rest-pose template mesh after adding shape- and pose-dependent deformations; $J(\beta)$ is the body-shape-dependent joint location; W is the skinning-weight matrix [30]; $BS\ (\beta;\ S)$ is the shape blend-shape function; β is the vector of linear shape coefficients; S represents the orthonormal principal components of vertex displacements used to capture shape variations due to individual differences; and $S = [S_1, \ldots, S_{|\beta|}] \in \mathbb{R}^{3N\times|\beta|}$is the matrix containing all such displacements.

The pose-dependent correction component is defined based on the difference between the rotation matrix of the current pose and that of the rest pose:

$$B_P(\theta;P) = \sum_{n=1}^{9K} \big(R_n(\theta) - R_n(\theta^*)\big) P_n \quad (3)$$

where $R(\theta)$ maps the pose vector to a sequence of relative rotation matrices between body segments, $R_n(\theta)$ denotes the nth element, θ* is the rest pose, and P_n is the principal component of pose-dependent deformation.

The facial-expression component is similarly described in a low-dimensional space:

$$B_E(\psi;E) = \sum_{n=1}^{|\psi|} \psi_n E_n \quad (4)$$

The 3D skeletal joint positions (J) are computed from the mesh vertices through a joint-regression matrix J:

$$J(\beta) = \mathcal{J}\big(\bar{T} + B_S(\beta;S)\big) \quad (5)$$

where the matrix J determines which mesh vertices contribute to the position of a specific joint [30].

For the hands, SMPL-X uses a low-dimensional Principal Component Analysis (PCA) space to reduce the number of parameters to be optimized:

$$\theta_h = \sum_{n=1}^{|m_h|} m_{h,n} M_n \quad (6)$$

To fit the 3D model to the two RGB images, the system minimizes the following generalized energy function $E(\beta,\theta,\psi)$:

$$E(\beta,\theta,\psi) = E_J + \lambda_{\theta_b}E_{\theta_b} + \lambda_{\theta_f}E_{\theta_f} + \lambda_{m_h}E_{m_h} +$$
$$+\lambda_\alpha E_\alpha + \lambda_\beta E_\beta + \lambda_E E_E + \lambda_C E_C \quad (7)$$

where, E_J is the data term based on the 2D reprojection error; E_{θ_b} is the body-pose prior; E_{θ_f}, E_{m_h}, E_β, and E_E are regularization terms for head pose, hand pose, body shape, and facial expression, respectively; E_α restricts abnormal flexion angles at the elbows and knees; and E_C is the interpenetration constraint between body surfaces.

A simple prior term for body shape is expressed as:

$$E_\beta(\beta) = \| \beta \|_2^2 \quad (8)$$

To keep the body shape as anatomically plausible and accurate as possible, the over-flexion constraint for the elbows and knees is expressed as follows:

$$E_\alpha(\theta_b) = \sum_{i\in\{\text{elbows,knees}\}} \exp(\theta_i) \quad (9)$$

The data error is computed as the robust distance between the 2D points detected in the image and the 2D projections of the corresponding 3D joints on the model:

$$E_J(\beta,\theta,K,J_{est}) = \sum_{\text{joint } i} \gamma_i\, \omega_i \rho\left(\Pi_K\left(R_\theta\big(J(\beta)\big)_i\right) - J_{est,i}\right) \quad (10)$$

where Π_K denotes the projection from 3D to 2D using the camera intrinsic parameters K; $R_\theta(.)$ transforms the joint according to the kinematic tree associated with the pose θ; $J_{est,i}$ is the estimated 2D joint; ω_i is the detection confidence; γ_i is the joint-specific weight used during optimization, and ρ is the robust Geman-McClure loss function, which reduces the influence of noisy detections [30].

2.3. Method for Measuring Anthropometric Dimensions from the Digital Human Model

From the 3D OBJ file, the human body model is represented as a mesh consisting of vertices and triangular faces. Before measurement, the model is normalized to the body coordinate system so that the vertical body axis is parallel to the global vertical axis. The body posture is adjusted to the neutral anatomical position to reduce errors due to postural deformation during anthropometric measurements.

Let I denote the input image. The recovered body-mesh model learns the mapping from the image to pose, shape, and camera parameters:

$$f(I) = (\theta, \beta, \psi, \pi) \quad (11)$$

The body model function $M(.)$ then generates the set of 3D body vertices:

$$V = M(\theta, \beta, \psi) \qquad V = \{v_j \in \mathbb{R}^3 \mid j = 1,2, \dots, N\} \quad (12)$$

where N is the number of mesh vertices. In SMPL-X, body deformation is commonly described by 99 pose parameters and 10 shape parameters [34, 36].

Before determining the dimensions, the model is sex-normalized and converted to the mean mesh in the A-pose to reduce the influence of postural differences on the measurement results.

For each anthropometric dimension to be measured, let P_i denote the corresponding measurement plane, with $i = 1,2, \dots, k$.

The set $\{P_i\}_{i=1}^{k}$ represents the predefined measurement planes for body dimensions such as chest, waist, hip, wrist, or shoulder:

$$\mathcal{P} = \{P_i \mid i = 1,2, \dots, k\} \quad (13)$$

Let T denote the reconstructed SMPL-X body surface. The vertex set or cutting curve used to measure the ith dimension is determined by the intersection between the body surface and the measurement plane:

$$M_i = T \cap P_i \quad (14)$$

In computational practice, M_i is represented by a sequence of neighboring vertices belonging to the measurement region [36]:

$$M_i = \left\{v_i^{(1)}, v_i^{(2)}, \dots, v_i^{(n_i)}\right\}, \qquad v_i^{(m)} \in T \quad (15)$$

where $v_i^{(m)}$ and $v_i^{(m+1)}$ are two adjacent vertices on the measurement curve. For circumferential dimensions, the measured value is computed as the sum of distances between consecutive vertex pairs along the closed cutting curve [36]:

$$L_i = \sum_{m=1}^{n_i} \left\| v_i^{(m)} - v_i^{(m+1)} \right\|_1, v_i^{(n_i+1)} = v_i^{(1)} \quad (16)$$

where $\|\cdot\|_1$ is the Manhattan norm, and the set of neighboring measurement segments on the cutting curve can be expressed as row-wise concatenation:

$$|M_i| = \left|v_i^{(1)} - v_i^{(2)}\right| \oplus \left|v_i^{(2)} - v_i^{(3)}\right| \oplus \cdots \oplus \left|v_i^{(m)} - v_i^{(n)}\right| \quad (17)$$

Where $\oplus$ is the row-wise concatenation operator. When a scalar anthropometric value is required, the component segments of $|M_i|$are summed to obtain the corresponding circumference or length.

For breadth dimensions, such as shoulder breadth, the measurement can be determined as the Euclidean distance between the left and right anatomical landmarks on the body mesh:

$$W_{shoulder} = \|p_L - p_R\|_2 \quad (18)$$

where $p_L$and p_R are the left and right shoulder landmarks, respectively. Unlike circumferential dimensions, breadth dimensions do not require tracing a closed cutting curve but require accurate identification of the corresponding landmarks on the mesh surface.

Body height is approximated from the bounding box of the reconstructed mesh. If $z_{\max}$ and $z_{\min}$ are the maximum and minimum coordinates, respectively, along the vertical direction of the vertex set, the geometric height of the model is calculated as follows:

$$H = z_{\max} - z_{\min} \quad (19)$$

When the model must be normalized to the subject's actual stature, the scale factor can be determined as:

$$s = \frac{H_{real}}{H_{mesh}} \quad (20)$$

Accordingly, all anthropometric dimensions obtained from the mesh are corrected as follows:

$$\hat{L}_i = sL_i \quad (21)$$

The output of the anthropometric measurement module is a set of body dimensions [16]:

$$\mathcal{A} = \left\{L_{chest}, L_{waist}, L_{hip}, L_{wrist}, W_{shoulder}, H, \dots\right\} \quad (22)$$

Based on the statistical data in Table 2, three body models corresponding to the minimum, mean, and maximum body sizes were selected [20].

The geometric dimensions measured for ergonomic assessment of driving comfort are presented as follows:

Table 2. Geometric dimensions of the three representative body models in the study dataset

No.	Parameter	Unit	Minimum size	Mean size	Maximum size
1	Height	cm	163.00	171.00	188.00
2	Body mass	kg	53.00	63.00	80.00
3	Sitting height	cm	86.39	90.63	99.64
4	Knee height	cm	42.63	46.70	51.14
5	Head length	cm	15.87	16.30	18.34
6	Head breadth	cm	14.57	15.78	16.70
7	Head height	cm	21.52	22.57	24.82
8	Shoulder breadth	cm	31.00	33.99	37.86
9	Chest circumference	cm	78.31	88.74	94.40
10	Chest depth	cm	20.81	21.66	26.13
11	Waist circumference	cm	65.86	76.03	90.16
12	Abdominal depth	cm	20.20	23.40	25.39
13	Hip circumference	cm	81.04	88.26	104.38
14	Thumb-tip reach	cm	71.88	73.56	74.28
15	Forearm length	cm	29.36	31.96	34.58
16	Hand length to wrist	cm	22.20	24.76	26.63
17	Hand breadth	cm	7.92	7.95	8.76
18	Hand depth	cm	2.84	2.88	2.89
19	Heel height	cm	6.80	7.43	8.32
20	Foot length	cm	21.58	24.14	26.59
21	Foot breadth	cm	8.57	9.54	9.92
22	Shoe height	cm	2.54	2.54	2.54

2.4. Development of Cabin Simulation and DHMs for Ergonomic Comfort Assessment using Siemens NX

To clarify the procedure for assessing driver ergonomic comfort, a simulation workflow was developed, as shown in the Figure 3. The workflow consists of four main steps: digital human model initialization, cabin simulation model development, DHM-cabin integration, and driving posture evaluation based on ergonomic criteria. This structured procedure enables a systematic analysis of driver–cabin interaction and supports the identification of ergonomic limitations as well as the optimization of key cabin design parameters.

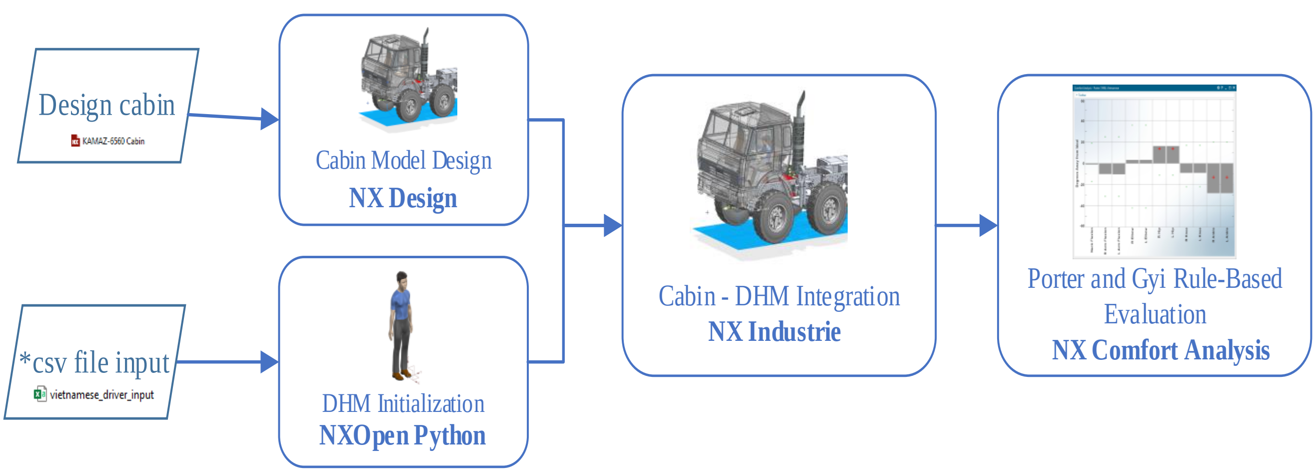

Fig. 3 Simulation workflow for driver ergonomic comfort assessment

2.4.1. 3D modeling and Simulation of the KAMAZ-6560 truck cabin

The NX software was used to simulate the KAMAZ-6560 truck cabin at a 1:1 scale in a 3D environment, enabling integration of the cabin model, seat, steering wheel, pedals, and main control components.

(a) (b) (c)

Fig. 4 General layout design of the specialized cabin using NX software: (a) Cabin reconstructed from 3D scanning data, (b) Cabin simulated in Siemens NX, and (c) Main cabin dimensions.

From the 3D cabin model, the main geometric dimensions were extracted to support spatial-layout evaluation and ergonomic compatibility assessment. Direct extraction of dimensions from the 3D model ensures consistency between the measured and the simulation data. These dimensions provide important input for analyzing driver posture and proposing cabin layout adjustments according to ergonomic requirements.

Table 3. Main geometric parameters of the cabin and its internal components

No.	Parameter	Symbol	Unit	Value
1	Distance between H-point and Accelerator Heel Point (AHP)	L1	mm	750
2	Distance between Steering Wheel Centre (SWC) and AHP	L2	mm	220
3	Clutch-pedal height relative to the vehicle floor	H1	mm	128
4	H-point height relative to the vehicle floor	H2	mm	408
5	SWC height relative to the vehicle floor	H3	mm	800
6	Angle between the seat back and the vertical direction	A1	degree	8
7	Angle between the steering wheel and the vertical direction	A2	degree	63
8	Angle between the clutch pedal and the vehicle floor	A3	degree	18

2.4.2. Establishing Vietnamese Anthropometric Parameters in the JACK Human Model

In Siemens NX, the JACK module enables the construction and simulation of human models in 3D space for ergonomic assessment and optimization of the working space inside the cabin. With the JACK model, designers can select detailed geometric dimensions, including height, body mass, arm span, field of vision, reach envelope, and joint range of motion, corresponding to each body segment (head, trunk, arms, and legs).

(a) (b) (c)

Fig. 5 JACK model with Vietnamese anthropometric parameters: (a) Vietnamese male, 20 years old, stature 163 cm, body mass 53 kg, (b) Vietnamese male, 20 years old, stature 171 cm, and (c) Vietnamese male, 20 years old, stature 188 cm, body mass 80 kg.

In particular, the JACK model allows anthropometric parameters to be adjusted for specific population groups, thereby enabling the input of a dataset representative of Vietnamese users. Consequently, the simulation can more accurately reflect sitting posture, visual field, operational reach, and driver comfort under actual operating conditions.

3. Results and Discussion

3.1. Investigation of Driving Comfort under Varying Anthropometric Parameters

To evaluate the ergonomic compatibility of the truck cabin with drivers of different body sizes, three digital human models representing the surveyed anthropometric group were positioned in the KAMAZ-6560 truck cabin model reconstructed from 3D scanning data. Comfort was assessed through the main joint angles of the model based on the comfort-angle limits reported in the ergonomic study by Porter and Gyi. The analysis results provide a basis for identifying incompatibilities in the original cabin layout with respect to the anthropometric characteristics of the surveyed Vietnamese group. The results are shown in Figure 6.

Figure 6 illustrates the deviation of the driver's joint angles from the comfort-angle range proposed by Porter and Gyi. A value of 0° indicates that the joint angle is within the comfort range; a positive value indicates that the joint angle exceeds the upper limit; and a negative value indicates that it is below the lower limit. From the statistical bar-chart evaluations, the main findings are as follows. In case (Figure 6a), the right and left arm-flexion angles both deviated by approximately 17.00°, indicating that the arms tended to be lower or more flexed than the comfort range, which may increase static shoulder loading during prolonged driving. In contrast, the neck, elbow, and knee angles showed only small deviations, indicating a relatively acceptable posture. A notable deviation occurred at the hip joint, with the maximum deviation from the ideal value reaching 17.79°. In this case, because the clutch pedal height was 12.80 cm, the mean foot length was approximately 23.00 cm, and the heel point was approximately 6.30 cm from the clutch pedal center, the largest deviation occurred at the ankle, approximately 28.01°, indicating excessive ankle flexion during pedal operation.

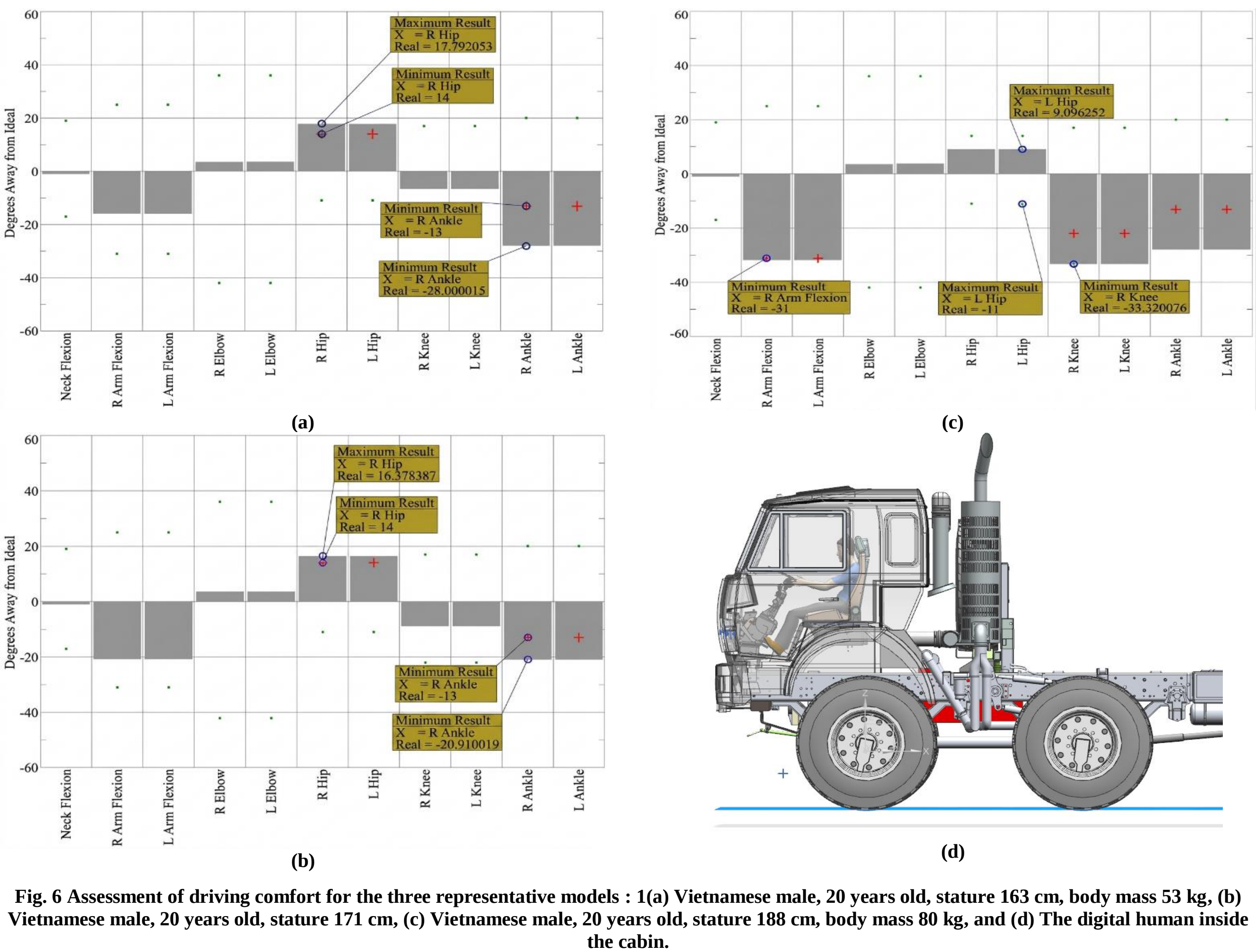

Fig. 6 Assessment of driving comfort for the three representative models : 1(a) Vietnamese male, 20 years old, stature 163 cm, body mass 53 kg, (b) Vietnamese male, 20 years old, stature 171 cm, (c) Vietnamese male, 20 years old, stature 188 cm, body mass 80 kg, and (d) The digital human inside the cabin.

For the Vietnamese model with a stature of 171.00 cm, the hip angle remained outside the comfort range by approximately 14.00-16.38°, similar to case (a); therefore, the seat-back angle can be adjusted to better match the sitting posture. As the driver's body height increased, particularly with a foot length of approximately 23.78 cm and a longer lower leg, clutch-pedal operation became easier. However, the ankle angle deviates from the comfort range by approximately 20.91°.

For the 188-cm-tall Vietnamese model, the seat position in the simulated cabin was shifted forward by approximately 10 cm, and the driver's neck and elbow angles remained within the comfort limits. However, the right and left arm angles showed large negative deviations of approximately 31°, indicating that the arms were excessively flexed or positioned too low relative to the recommendation. For this body size, the knee angle exceeded the comfort limit by approximately 10.00°, suggesting that the seat height should also be adjusted to keep the knee angle within the allowable range; the seat should be raised by approximately 8.00 cm. Although this model was larger than those in the two preceding cases, the current cabin geometry still resulted in a less-than-optimal sitting posture, causing the ankle angle to exceed the allowable limit by approximately 12.00°.

Based on these results, to achieve a comfortable ankle angle during clutch-pedal operation, the clutch pedal should be lowered so that the main force-application point is located in the forefoot region. With a mean foot length of approximately 24.00 cm, a maximum comfortable foot-ankle angle of 113.00°, and a foot inclination of approximately 23.00° relative to the horizontal plane, the height from the floor to the clutch-pedal contact point should be within 7-8 cm. Overall, the main ergonomic limitations are concentrated in the arms, knees, and ankles, indicating that the steering-wheel position, seat, and pedal assembly should be adjusted to bring the driving posture closer to the comfort range.

4. Conclusion

This study focuses on developing a digital human model using a two-dimensional image-based body-shape estimation method, validated against actual body dimensions to improve accuracy and accelerate the anthropometric data acquisition process. In conventional anthropometric surveys, investigators must carefully measure the body and manually record each parameter. By contrast, using only two images captured from the frontal and lateral views, a three-dimensional digital model can be reconstructed with the complete geometric parameters of the representative subject. This enables the digitization of anthropometric data, thereby making data storage, management, and reuse more convenient and efficient. Along with the rapid development of computer-aided design technologies, the ability to model the human body with anthropometric characteristics specific to the Vietnamese population is of significant scientific value, particularly for domestic automotive design in general and driver-oriented ergonomic design in particular. Such a model can help designers substantially reduce the time and cost required for physical testing, while accelerating the evaluation and development of new cabin prototypes. It also helps minimize common cabin-design shortcomings, such as restricted driver visibility, overly compact and confined design spaces, insufficient comfort, and unfavorable working conditions that may cause driver fatigue and loss of concentration. Furthermore, this study provides recommendations regarding the positioning and adjustment ranges of the clutch pedal, driver seat, and steering wheel for a specific specialized cabin configuration. These findings contribute to improving the methodology for assessing driver ergonomic comfort by integrating digital human models with simulated cabin models.

Future work will focus on three-dimensional object scanning and computer vision methods to develop digital human models with higher accuracy, expected to be in the range of 0.5-2.0%. In comparison, the two-dimensional image-based estimation method used in this study yields surface errors in the range of approximately 1.5-3.0%. In addition, the present study was limited to a sample of male participants aged 20-29 years. Therefore, future research should expand both the sample size and the target population to include Vietnamese males and females, particularly those of working age. This would provide a more comprehensive basis for establishing a Vietnamese human digital model library applicable to design tasks across various fields of daily life.

Conflicts of Interest

The authors declare that there is no conflict of interest regarding the publication of this paper.

Funding Statement

This research received no specific grant from any funding agency in the public, commercial, or not-for-profit sectors.

Acknowledgments

The authors would like to acknowledge the support of Le Quy Don Technical University during this study.

References

[1] Ngo Xuan Khoa et al., "Several Dimensions, Anthropometric Indices and Nutritional Condition of Freshmen in Hanoi Medical University, Year 2019-2020," *Vietnam Medical Journal*, vol. 506, no. 1-2, pp. 1-7, 2021. [CrossRef] [Google Scholar] [Publisher Link]

[2] Huy G. Nguyen et al., "Reference Values of Body Composition Parameters for Vietnamese Men and Women," *European Journal of Clinical Nutrition*, vol. 75, pp. 1283-1290, 2021. [CrossRef] [Google Scholar] [Publisher Link]

[3] Pham Thi Bich Ngan et al., "General Comments on Anthropometric Characteristics of Vietnamese in their Working Age in 2018-2019," *Journal of Occupational Safety, Health & Environment Activities*, 2019. [Publisher Link]

[4] Nguyen Tan Gi Trong, *Biological Constants of Vietnamese People*, Medical Publishing House, pp. 1-151, 1975. [Publisher Link]

[5] Hung Vo, *Anthropometric Atlas of Vietnamese in their Working Age: Data and Instructions for Use*, Vietnam General Confederation of Labour, and Institute of Occupational Safety and Health Sciences, Science and Technics Publishing House, pp. 1-155, 1986. [Publisher Link]

[6] Anh Kim Dang et al., "Anthropometric Cut-Off Values for Detecting the Presence of Metabolic Syndrome and Its Multiple Components among Adults in Vietnam: The Role of Novel Indices," *Nutrients*, vol. 14, no. 19, pp. 1-14, 2022. [CrossRef] [Google Scholar] [Publisher Link]

[7] Heiner Bubb et al., *Automobilergonomie*, Springer Vieweg Wiesbaden, 2015. [CrossRef] [Google Scholar] [Publisher Link]

[8] Mong Hien Thi Nguyen et al., "The Algorithm to Automatically Extract Body Sizes and Shapes," *Textile Worker*, vol. 65, no. 1, pp. 67-80, 2022. [CrossRef] [Google Scholar] [Publisher Link]

[9] Dat Tien Nguyen, and Thach Ngoc Hoang, "3D Reconstruction Human Body from Anthropometric Measurements Using Diversity Control Oriented Genetic Algorithm," *Mendel*, vol. 27, no. 1, pp. 49-57, 2021. [CrossRef] [Google Scholar] [Publisher Link]

[10] Thi Minh Kieu Tran, Mau Tung Nguyen, and Thi Van Anh Tran, "Classification of Body Types of Vietnamese Middle-Aged Men in Ho Chi Minh City," *Engineering and Technology for Sustainable Development*, vol. 32, no. 5, pp. 28-36, 2022. [CrossRef] [Google Scholar] [Publisher Link]

[11] Hoang Thi Yen, Phan Nguyen Uyen Nguyen, and Mong Hien Thi Nguyen, "Analysis and Modeling of Adult Male Body Shape Aged 25–45 by CLO3D Software," *BOHR International Journal of Computer Science*, vol. 3, no. 1, pp. 1-11, 2024. [CrossRef] [Google Scholar] [Publisher Link]

[12] Tran Thi Minh Kieu et al., "Analysis of Vietnamese Women's Body Shape from Anthropometric Data," *Fibres and Textiles*, vol. 31, no. 1, pp. 1-10, 2024. [CrossRef] [Google Scholar] [Publisher Link]

[13] Russell Marshall et al., "Advances in Digital Human Modeling II," *Proceedings of the 9th International Digital Human Modeling Symposium, DHM 2025* Loughborough, UK, vol. 1577, 2025. [CrossRef] [Publisher Link]

[14] A.B Rathod, and R.T Vyavahare, "Design Optimization of Truck Cabin for Driver Comfort," *Research Square*, pp. 1-23, 2025. [CrossRef] [Google Scholar] [Publisher Link]

[15] A.B. Rathod, and R.T. Vyavhare, "Optimization of Truck Driver Cab Ergonomic for Commercial Truck Based on Ramsis: Enhancing Driver Comfort and Safety," *International Journal of Intelligent Transportation Systems Research*, vol. 22, no. 3, pp. 603-613, 2024. [CrossRef] [Google Scholar] [Publisher Link]

[16] Marco Freddi, Curzio Pagliari, and Leonardo Frizziero, "Optimizing Driver Position Using ANOVA and ANNs," *IEEE Access*, vol. 13, pp. 166436-166443, 2025. [CrossRef] [Google Scholar] [Publisher Link]

[17] Matthew B. Parkinson et al., "Optimizing Truck Cab Layout for Driver Accommodation," *Journal of Mechanical Design*, vol. 129, no. 11, pp. 1110-1117, 2007. [CrossRef] [Google Scholar] [Publisher Link]

[18] Junfeng Peng, Xuguang Wang, and Lisa Denninger, "Effects of Anthropometric Variables and Seat Height on Automobile Drivers' Preferred Posture with the Presence of the Clutch," *Human Factors: The Journal of the Human Factors and Ergonomics Society*, vol. 60, no. 2, pp. 172-190, 2018. [CrossRef] [Google Scholar] [Publisher Link]

[19] Junfeng Peng, Xuguang Wang, and Lisa Denninger, "Ranges of the Least Uncomfortable Joint Angles for Assessing Automotive Driving Posture," *Applied Ergonomics*, vol. 61, pp. 12-21, 2017. [CrossRef] [Google Scholar] [Publisher Link]

[20] Baba Md Deros et al., "Incorporating Malaysian's Population Anthropometry Data in the Design of an Ergonomic Driver's Seat," *Procedia - Social and Behavioral Sciences*, vol. 195, pp. 2753-2760, 2015. [CrossRef] [Google Scholar] [Publisher Link]

[21] Esteban Ortiz et al., "Evaluation of Technical and Anthropometric Factors in Postures and Muscle Activation of Heavy-Truck Vehicle Drivers: Implications for the Design of Ergonomic Cabins," *Applied Sciences*, vol. 15, no. 14, pp. 1-16, 2025. [CrossRef] [Google Scholar] [Publisher Link]

[22] J. Mark Porter, and Diane E. Gyi, "Exploring the Optimum Posture for Driver Comfort," *International Journal of Vehicle Design*, vol. 19, no. 3, pp. 255-266, 1998. [CrossRef] [Google Scholar] [Publisher Link]

[23] Julian Happian-Smith, "An Introduction to Modern Vehicle Design," *Butterworth-Heinemann*, 2002. [Google Scholar] [Publisher Link]

[24] H. Onan Demirel, Salman Ahmed, and Vincent G. Duffy, "Digital Human Modeling: A Review and Reappraisal of Origins, Present, and Expected Future Methods for Representing Humans Computationally," *International Journal of Human-Computer Interaction*, vol. 32, no. 10, pp. 897-937, 2022. [CrossRef] [Google Scholar] [Publisher Link]

[25] Don B. Chaffin, "Digital Human Modeling for Workspace Design," *Reviews of Human Factors and Ergonomics*, vol. 4, no. 1, pp. 41-74, 2008. [CrossRef] [Google Scholar] [Publisher Link]

[26] Kihyo Jung, Ochae Kwon, and Heecheon You, "Development of a Digital Human Model Generation Method for Ergonomic Design in Virtual Environment," *International Journal of Industrial Ergonomics*, vol. 39, no. 5, pp. 744-748, 2009. [CrossRef] [Google Scholar] [Publisher Link]

[27] Qiqi He et al., "From Digital Human Modeling to Human Digital Twin: Framework and Perspectives in Human Factors," *Chinese Journal of Mechanical Engineering*, vol. 37, no. 1, pp. 1-14, 2024. [CrossRef] [Google Scholar] [Publisher Link]

[28] Sunghee Lee, Eftychios Sifakis, and Demetri Terzopoulos, "Comprehensive Biomechanical Modeling and Simulation of the Upper Body," *ACM Transactions on Graphics*, vol. 28, no. 4, pp. 1-17, 2009. [CrossRef] [Google Scholar] [Publisher Link]

[29] Ali Hamadi Dicko, "*Construction of Musculoskeletal Systems for Anatomical Simulation*," Doctoral thesis, University of Grenoble, 2014. [CrossRef] [Google Scholar] [Publisher Link]

[30] Matthew Loper et al., "SMPL: A Skinned Multi-Person Linear Model," *Seminal Graphics Papers: Pushing the Boundaries*, vol. 2, pp. 851-866, 34, no. 6, pp. 1-16, 2023. [CrossRef] [Google Scholar] [Publisher Link]

[31] Patrick Lerge et al., "Definition of the Neutral Body Posture through Three-Dimensional Local Cardan Joint Angles," *Acta Astronautica*, vol. 244, pp. 323-334, 2026. [CrossRef] [Google Scholar] [Publisher Link]

[32] Zhongguo Li, Magnus Oskarsson, and Anders Heyden, "3D Human Pose and Shape Estimation Through Collaborative Learning and Multi-view Model-fitting," *2021 IEEE Winter Conference on Applications of Computer Vision (WACV)*, Waikoloa, HI, USA, pp. 1887-1896, 2021. [CrossRef] [Google Scholar] [Publisher Link]

[33] Gyungin Jung, Minjoo Kang, and Sungmin Kim, "Development and Evaluation of Accurate 3D Human Models using Scan Data: A Comparison with SMPL and CLO Models," *Fashion and Textiles*, vol. 12, pp. 1-17, 2025. [CrossRef] [Google Scholar] [Publisher Link]

[34] Yidong Wu, "3D Human Body Model Reconstruction Algorithm Based on Multi-View Synchronized Video Sequences," *Proceedings of the 2nd International Conference on Data Analysis and Machine Learning (DAML)*, Kuala Lumpur, Malaysia, vol. 1, pp. 214-220, 2024. [CrossRef] [Google Scholar] [Publisher Link]

[35] David Bojanić et al., "Pose-Independent 3D Anthropometry from Sparse Data," *European Conference on Computer Vision*, pp. 237-256, 2024. [CrossRef] [Google Scholar] [Publisher Link]

[36] Shuhang Chen et al., "A Focused Human Body Model for Accurate Anthropometric Measurements Extraction," *2025 IEEE/CVF Conference on Computer Vision and Pattern Recognition (CVPR)*, Nashville, TN, USA, pp. 22658, 22667, 2025. [CrossRef] [Google Scholar] [Publisher Link]

[37] Katja Ludwig et al., "Leveraging Anthropometric Measurements to Improve Human Mesh Estimation and Ensure Consistent Body Shapes," *2025 IEEE/CVF Conference on Computer Vision and Pattern Recognition Workshops (CVPRW)*, Nashville, TN, USA, pp. 5862-5871, 2025. [CrossRef] [Google Scholar] [Publisher Link]

[38] Ke Ke Sun et al., "A 2D-3D Non-Contact Anthropometric Method for Daily Dressing State-Takes Young Asian Women as Example," *Journal of Measurements in Engineering*, vol. 5, no. 3, pp. 161-175, 2017. [CrossRef] [Google Scholar] [Publisher Link]

[39] A. Ballester et al., "3D Human Models from 1D, 2D & 3D Inputs: Reliability and Compatibility of Body Measurements," *Proceedings of the 9th International Conference and Exhibition on 3D Body Scanning and Processing Technologies*, Lugano, Switzerland, pp. 132-141, 2018. [CrossRef] [Google Scholar] [Publisher Link]